Influence of Stochastic Geometric Imperfection on the Ultimate Strength of Stiffened Panel in Compression

D.G. Georgiadis & M.S. Samuelides
School of Naval Architecture and Marine Engineering, National Technical University of Athens, Greece

S. Li
Department of Naval Architecture, Ocean and Marine Engineering, University of Strathclyde, Glasgow, UK

D.K. Kim & S. Benson
Group of Marine, Offshore and Subsea Technology, School of Engineering, Newcastle University, UK

ABSTRACT: The initial geometric imperfection is recognized as substantially influential on the buckling behaviour and ultimate strength of stiffened plated structures. Conventionally, the initial geometric imperfection is defined in a deterministic manner, such as a hungry-horse mode, ARE mode or critical buckling mode with characteristic magnitudes. However, due to the uncertainty in manufacturing and in-service effects, the initial geometric imperfection should be better described as a random field. This paper aims to assess the effects of the stochastic nature of geometric imperfection on the ultimate strength of stiffened panel in compression. A probabilistically-based imperfection model developed by spectral representation method is applied to an orthogonally stiffened panel. A Monte-Carlo Simulation enhanced by a Latin-Hypercube Scheme (LHS) is utilized to sample the initial geometric imperfection. A series of nonlinear finite element analyses are completed to calculate the ultimate compressive strength of the case study model. With reference to the deterministic representations, the impact of the stochastic imperfection model is discussed. The present work may provide useful insights for the reliability-based ship structural assessment regarding the uncertainty due to geometric imperfection.

1 INTRODUCTION

The stiffened panel is the most common load-carrying component of ship structures against various environmental loads, such as the in-plane compression induced by longitudinal bending. The assessment of stiffened panel's adequacy to withstand the longitudinal compression could be based on an ultimate limit state (ULS) criterion (Paik, 2019; 2020). To complete the ULS assessment, a rational evaluation of the ultimate compressive strength of stiffened panels is necessary.

In the shipbuilding industry, a stiffened panel is usually assembled from plating and stiffeners by welding. This will inevitably induce imperfections on the assembled structures in the form of geometric distortion and residual stress (Li et al., 2021). As shown by many studies, the initial geometric imperfection is one of the most important parameters of influence in the assessment of elastoplastic buckling and ultimate strength performance of stiffened plated structures (Smith, 1981; 1987; 1991).

The geometric imperfection of ship-type stiffened panels is conventionally defined in a deterministic way. Typical distortion profiles include the hungry-horse (HH) mode, Admiralty Research Establishment (ARE) mode and critical buckling (CB) mode. The HH mode was developed based on the full-scale measurement on various merchant ships (Ueda and Yao, 1985). The ARE mode was originally introduced by the British Navy in a semi-empirical way and was recently refined by Benson (2011). The CB mode is the simplest form of imperfection and is widely adopted in the literature such as the ISSC (2012), Paik et al. (2004) and Gordo (2015). In civil engineering, the CB mode was also recommended by Merrison Committee (1973) for bridge structures. Regarding the maximum distortion magnitude, various characteristics values were introduced (Smith et al., 1987; Dowling et al., 1973; Antoniou, 1980; Kmiecik, 1981; Carlsen and Czujko, 1978). Among these, the recommendation by Smith et al. (1987) is the most commonly accepted, which includes three levels of severity, i.e. slight, average and severe. Except as otherwise specified, the most usual practice in the ultimate strength calculation of ship structures is to model the geometric imperfection based on one of the aforementioned distortion profiles and to assume an average-level magnitude. Recently, there was an application of photogrammetry technique to measure the geometric imperfection for structural analysis (Woloszyk et al., 2021).

However, due to the uncertainties in manufacturing and in-service effects, the geometric imperfection is partially random in its profile and magnitude. Thus, it would be more rational to represent the geometric

imperfection as a random field. In the light of this, a probabilistic study is presented in this paper to investigate the influence of stochastic geometric imperfection on the ultimate strength of stiffened panel. A probabilistically-based imperfection model developed by the spectral representation method is applied to an orthogonally stiffened panel. The sampling of geometric imperfection is enabled by a Monte-Carlo Simulation enhanced by a Latin-Hypercube scheme. A series of nonlinear finite element analyses are carried out to calculate the ultimate compressive strength statistics of the case study model. By comparison with the deterministic representations, the impact of the stochastic imperfection model is discussed.

2 BACKGROUND

2.1 *Deterministic shape of geometric imperfection*

The general expressions of the deterministic geometric imperfection profiles (i.e. HH mode, ARE mode and CM mode) are given by Equation (1) to Equation (3) respectively. A comparison of these imperfection profiles is shown in Figure 1 for ship plates with aspect ratio $a/b = 2$ and $a/b = 5$.

Hungry-horse (HH) mode:

$$w_{opl} = w_{opl}^{max} \sum_{i=1}^{11} A_{0i} sin\left(\frac{i\pi x}{a}\right) sin\left(\frac{\pi y}{b}\right) \quad (1)$$

Admiralty Research Establishment (ARE) mode:

$$w_{opl} = w_{opl}^{max} \left\{A_1 sin\left(\frac{\pi x}{a}\right) + A_j sin\left(\frac{j\pi x}{a}\right) + A_{j+1} sin\left[\frac{(j+1)\pi x}{a}\right]\right\} sin\left(\frac{\pi y}{b}\right) \quad (2a)$$

$$j = a/b + 1 \quad (2b)$$

$$A_1/A_j = 4.0 \quad (2c)$$

$$A_{j+1} = 0.01 \quad (2d)$$

Critical buckling (CM) mode:

$$w_{opl} = w_{opl}^{max} sin\left(\frac{m\pi x}{a}\right) sin\left(\frac{\pi y}{b}\right) \quad (3a)$$

$$a/b \leq \sqrt{m(m+1)} \quad (3b)$$

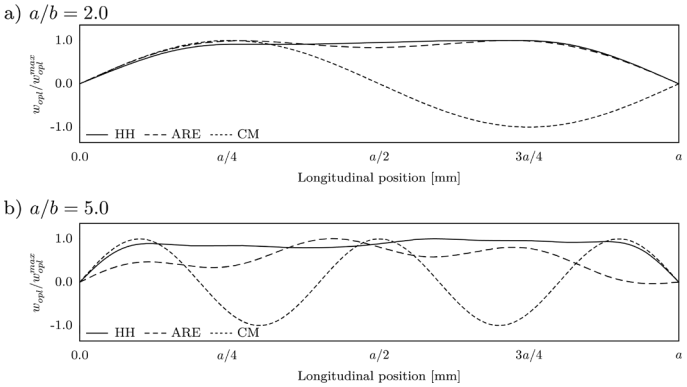

Figure 1. Comparison of typical deterministic geometric imperfection profiles

The HH mode was developed based on the measurements by Ueda and Yao (1985). Regression analysis with eleven Fourier components is applied to the collected data. The derived coefficients of each Fourier component are given in the appendix (Table A1). A recent full-scale measurement by Yi et al. (2020) further confirms the validity of a hungry-horse mode shape induced by the common welding technique in shipyards. However, as shown in Figure 1, the HH mode is typically in a barrel form, in which case a sudden change in the buckling mode may occur. This phenomenon could impose some difficulties in numerical simulation. The application of this imperfection model is presented by Tanaka et al. (2014).

The ARE mode is a semi-empirical imperfection representing a "real" plate whilst ensuring that the plate buckling will nucleate into an appropriate pattern. Three imperfection modes are superimposed to define the complete profile, in which the first two modes (i.e. A_1 and A_j) represent a combination of realistic distortion and critical buckling, while the high-order mode (A_{j+1}) ensures that the nucleation of out-of-plane deflection occurs at one part of the plate. The ratio between A_1 and A_j as specified by Equation (2c) is introduced based on measurements, which is also in agreement with the data reported by Carlsen and Czujko (1978). Typical values of A_1 and A_j are given in the appendix (Table A2) for different aspect ratios. Applications of this imperfection model are presented by Benson et al. (2015) and Li et al., (2019; 2020).

The CM mode is only constituted by one sinusoidal function, which is the preferred buckling mode of the tested plating. In numerical simulation based on CM mode, the distortion of the plating would generally follow the initial shape up to, and probably beyond the ultimate collapse. The CM mode may result in an overly conservative estimation of the ultimate strength of plates and stiffened panels. Moreover, a significant distortion could occur from the beginning of the compressive load application, which causes an underestimation of the in-plane stiffness of the panels, as compared with the other two mode shapes. However, the CM mode could help avoiding the convergence issue of numerical analysis, which is particular useful for the analysis of large-scale structures. Applications of this imperfection model are presented by ISSC (2012), Kim et al. (2017; 2019; 2020), Li and Benson (2019).

2.2 *Deterministic magnitude of geometric imperfection*

Once the deterministic shape of the geometric distortion is defined, the maximum amplitude of the distortion field should be specified. The recommendation by Smith et al. (1987) is given by Equation (4) in terms of plate slenderness ratio β and thickness t.

$$w_{opl}^{max} = 0.025\beta^2 t \text{ (slight)} \quad (4a)$$

$$w_{opl}^{max} = 0.100\beta^2 t \text{ (average)} \quad (4b)$$

$$w_{opl}^{max} = 0.300\beta^2 t \text{ (severe)} \quad (4c)$$

3 METHODOLOGY

3.1 *Overview*

The overall methodology of the numerical analysis of the ultimate compressive strength of stiffened panel with stochastic geometric imperfection is illustrated by the flowchart of Figure 2. Broadly speaking, with the aid of Monte-Carlo sampling, different geometric imperfections are generated and applied to the finite element model. In the following, a concise introduction is given for the fundamentals of the stochastic geometric imperfection.

3.2 *Stochastic geometric imperfection*

A stochastic geometric imperfection model was proposed by Georgiadis and Samuelides (2021) for local plating. As shown in Figure 3, the random field is introduced based on an effective length a_{eff}. The geometric imperfection w_{eff} along the effective length is given by Equation (5) where w_o is the mean imperfection magnitude and $\hat{f}(x)$ is a zero-mean Gaussian stochastic field. The full description along the centerline of the local plate is given by Equation (6).

$$w_{eff}(x) = w_0 + \hat{f}(x) \quad (5)$$

For $0 \le x \le a_0$

$$w_{opl}(x) = w_{eff}(x = x_0)|sin(\pi x/2a_0)| \quad (6a)$$

For $a_0 \le x \le a_1 + a_{eff}$

$$w_{opl}(x) = w_{eff}(x) \quad (6b)$$

For $a_1 + a_{eff} \le x \le a$

$$w_{opl}(x) = w_{eff}(x = x_1)\left|sin\left[\pi\left(x - a_{eff}\right)/2a_0\right]\right| \quad (6c)$$

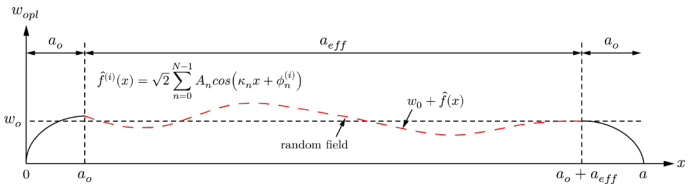

Figure 3. Schematics of stochastic geometric imperfection

For determining the effective length a_{eff}, Equation (7) or Equation (8) can be applied. The former was used by Dow and Smith (1984) and the latter was adopted by Ueda and Yao (1985).

$$a_{eff} = a - 2a_0 = 0.80a \quad (7)$$

$$a_{eff} = a - 2a_0 = 0.50a \ \ for\ \sqrt{2} \le a/b \le \sqrt{6} \quad (8a)$$

$$a_{eff} = a - 2a_0 = 0.67a \ \ for\ \sqrt{6} \le a/b \le \sqrt{12} \quad (8b)$$

$$a_{eff} = a - 2a_0 = 0.75a \ \ for\ \sqrt{12} \le a/b \le \sqrt{20} \quad (8c)$$

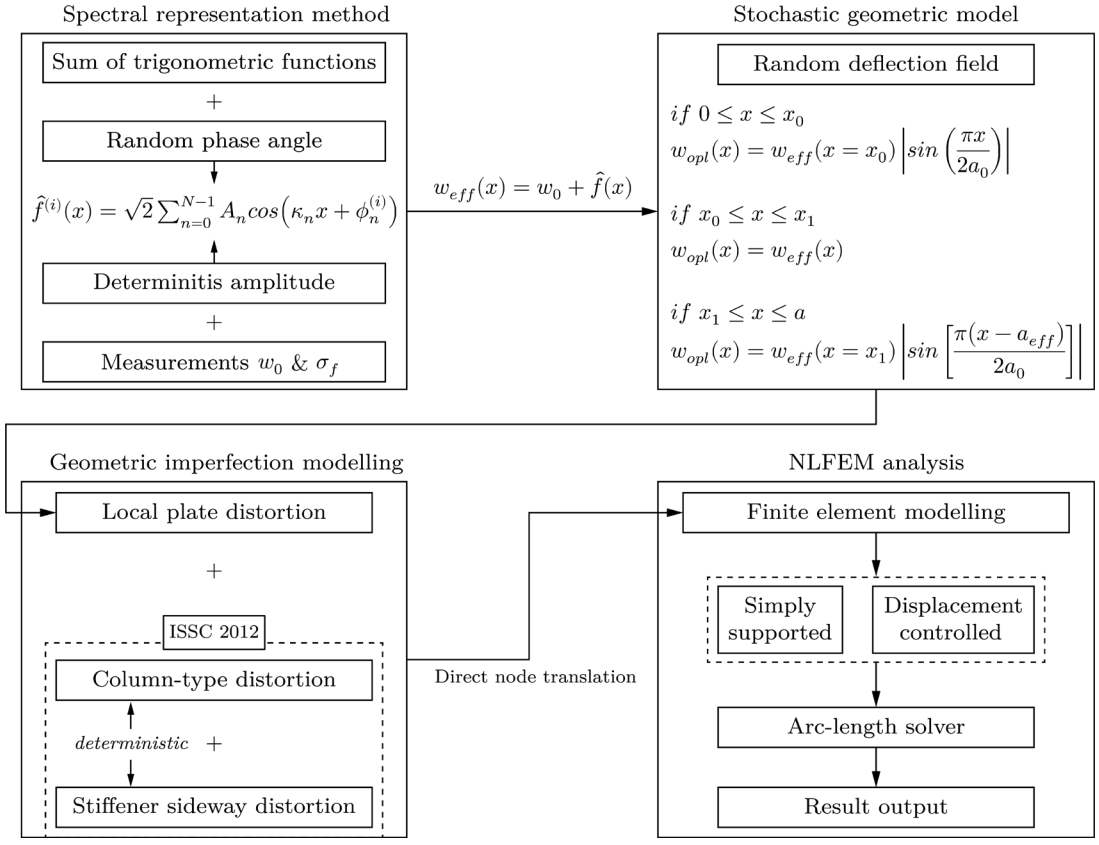

Figure 2. Flowchart of the proposed methodology

A random realization (i) of the stochastic field $\hat{f}(x)$ is generated from Equation (9) as a sum of cosine series with deterministic amplitudes A_n and random phase angles φ_n (Shinozuka and Deodatis, 1991).

$$\hat{f}^{(i)}(x) = \sqrt{2}\sum_{n=0}^{N-1} A_n \cos\left(\kappa_n x + \phi_n^{(i)}\right) \tag{9a}$$

$$A_n = \sqrt{2S_{ff}(\kappa_n)\Delta\kappa}, \text{ for } n = 0,1,\cdots,N-1 \tag{9b}$$

$$\kappa_n = n\Delta\kappa = \kappa_u/N \tag{9c}$$

$$A_0 = 0 \tag{9d}$$

Equation (9d) is imposed to ensure that the spatial average and autocorrelation function of any sample function $\hat{f}^{(i)}(x)$ are identical to the corresponding targets. The term κ_u denotes the upper cut-off wave number which defines the active region of the power spectrum S_{ff}. The step dx of the generated sample functions must satisfy the condition $dx \leq \pi/\kappa_u$ to avoid aliasing.

In this study, the number of terms in the cosine series is chosen as $N = 128$, which is sufficient to ensure some level of convergence to Gaussianity through the central limit theorem (Stefanou 2009). The stochastic field $\hat{f}(x)$ is assumed as homogenous and Gaussian. The (weakly) homogeneity concept implies a constant mean value and an autocorrelation form that can be expressed as a function of the relative distance between locations. As discussed by Georgiadis and Samuelides (2021), actual measurements on plates of merchant ships indicate that the above two conditions are satisfied. The normality concept can also be verified by the actual measurements. This is demonstrated in Figure 4, where a good agreement between the measurements of initial deflections for plates of similar characteristics with a normal distribution has been observed.

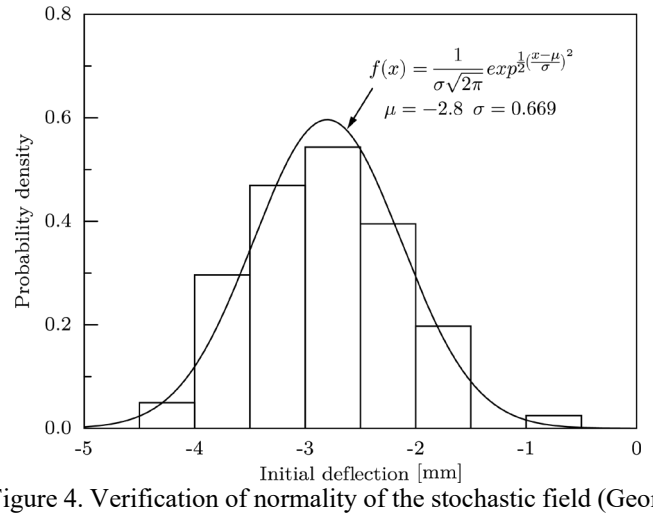

Figure 4. Verification of normality of the stochastic field (Georgiadis and Samuelides 2021)

Using Fourier transformation, the power spectral density $S_{ff}(\kappa)$ is given by Equation (10) where R_{ff} is the autocorrelation function representing the dependence between two arbitrary locations. The autocorrelation function adopted in this paper is given by Equation (11) where σ_f denotes the standard deviation of the stochastic field, $|\tau|$ is the absolute relative distance between two locations and l_c is the correlation length parameter. The correlation length l_c is chosen as 1700mm for the present paper. As examined by the preliminary evaluation, the adopted correlation length would generate reasonable geometric imperfection without excessive noise.

$$S_{ff}(\kappa) = \frac{1}{\pi}\int_0^\infty R_{ff}(\tau)\cos(\kappa\tau)d\tau \tag{10}$$

$$R_{ff} = \sigma_f^2\rho_{ff}(\tau) = \sigma_f^2\frac{l_c^4(l_c^2-3|\tau|^2)}{(l_c^2+|\tau|^2)^3} \tag{11}$$

A Monte-Carlo simulation enhanced by the Latin-Hypercube sample (Figure 5) is adopted to generate different geometric imperfections for the local plating, which is applied to the finite element model of the tested panel for computing the ultimate compressive strength. The Latin-Hypercube Scheme (LHS) is useful for efficiently selecting probable scenarios from multiple variables. Applications of this technique in the probabilistic study of ships and offshore structural strength include Paik et al. (2012), Kim et al. (2013; 2020), Youssef et al. (2016), Wong and Kim (2018) and Paik et al. (2019).

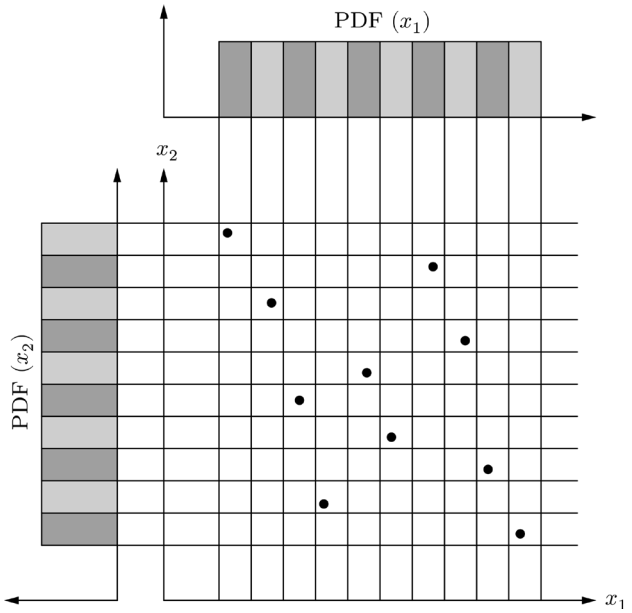

Figure 5. Latin-Hypercube sampling

4 CASE STUDY

4.1 *Premise*

A multi-frame orthogonally stiffened panel is adopted for case study (Figure 6). This stiffened panel was experimentally tested by Smith (1975). The principal of the case study model is listed in Table 3.

Table 3. Principal of the case study panel

Local plating	a [mm]	b [mm]	t_p [mm]	
	1219.2	609.6	8.0	
Long. stiffener	h_w [mm]	t_w[mm]	b_f [mm]	t_f [mm]
	153.7	7.2	79.0	14.2
Trans. frame	h_w [mm]	t_w[mm]	b_f [mm]	t_f [mm]
	257.6	9.3	135.0	18.3
Material (Plate)	σ_Y [MPa]		E [GPa]	
	226.1		184.156	
Material (Long.)	σ_Y [MPa]		E [GPa]	
	230.3		158.680	
Material (Trans.)	σ_Y [MPa]		E [GPa]	
	255.1		158.680	

For the finite element modelling, four-node shell element with reduced integration available in ABAQUS is employed. Each local plating is discretized by 24 elements longitudinally and 12 elements transversely. For longitudinal stiffeners, all webs and flanges are subdivided into 6 elements. In terms of the transverse frame, a compatibly coarse meshing scheme is applied. Simple support boundary condition is assumed. The vertical and transverse displacement at the loaded edge are constrained while only the vertical displacement is constrained at the unloaded long edge. The edge compression is applied through displacement-controlled technique. The geometric imperfection is applied by a direct-node translation approach (Benson et al., 2012). Apart from the local plate imperfection, deterministic column-type (Equation 12) and stiffener sideway imperfections (Equation 13) are also introduced to the finite element model. Note that the parameter B in Equation (12) refers to the width of the whole panel. For all imperfections, the relative distortion between the adjacent panel is of an asymmetric shape.

The test matrix is summarized in Table 4, which includes 36 analyses based on the deterministic imperfection and 100 samples generated by the stochastic geometric imperfection model. With the deterministic geometric shapes, the maximum distortion magnitude is varied from $0.025\beta^2 t$ to $0.3\beta^2 t$ at an increment of $0.025\beta^2 t$ assuming an uniform distribution. Regarding the stochastic model, the mean distortion and its standard deviation are specified as $0.006b$ and $0.00264b$ in accordance with the experimental measurement, which are equivalent to $0.064\beta^2 t$ and $0.028\beta^2 t$ respectively.

$$w_{oc} = w_{oc}^{max} sin\left(\frac{\pi x}{a}\right) sin\left(\frac{\pi y}{B}\right) \quad (12)$$

$$w_{os} = w_{os}^{max} \frac{z}{h_w} sin\left(\frac{\pi x}{a}\right) \quad (13)$$

$$w_{oc}^{max} = w_{os}^{max} = 0.0015a \quad (14)$$

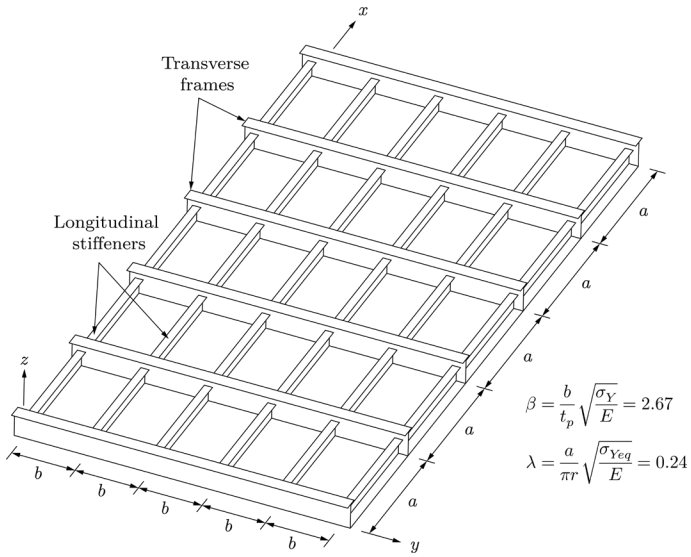

Figure 6. Schematics of the case study stiffened panel

Table 4. Test matrix

	Profile	Magnitude
Deterministic (3 × 12)	HH*	$0.025\beta^2 t$~$0.3\beta^2 t$
	ARE*	$0.025\beta^2 t$~$0.3\beta^2 t$
	CM*	$0.025\beta^2 t$~$0.3\beta^2 t$
Stochastic (× 100)	Proposed**	$w_0 = 0.064\beta^2 t$ $\sigma_f = 0.028\beta^2 t$

* Uniform distribution; ** Normal distribution

4.2 *Results and discussions*

The comparison of the computed ultimate compressive strength (mean and variance) is shown in Figure 7 for different imperfection models. Figure 8 illustrates the relationship between the maximum distortion magnitude and the ultimate compressive strength of stiffened panel, assuming deterministic imperfection shape. A number of insights are developed from the analyses:

- As demonstrated by Figure 7, the ultmiate compressive strength predictions of stiffened panel well correlate with the experimental measuremnt for all imperfection models, demonstrating that the stochastic imperfection model is a capable alternative as compared with the existing deterministic approach. The prediction based on HH mode has the largest mean value, which is likely attributed for the unified maximum distortion magnitude in all local plates.
- With the use of deterministic imperfection models, it is not necessarily true that a larger maximum distortion magnitude would lead to a reduction of the ultimate compressive strength, such as the ARE mode and HH mode in Figure 8. This is likely due to the coupling between the different deflection components. The deflection

component other than the preferred buckling mode has a strengthening effect on the stiffened panel, as it would suppress the development of out-of-plane deflection. As shown in Figure 9, with a higher maximum magnitude, the single half-wave component increases during the entire progressive collapse process. This results in a smaller deflection in a critical buckling mode, which therefore leads to an increase of the ultimate strength.

- Structural performance inspection based on the maximum distortion magnitude could therefore be misleading, since it omits the coupling effect between the imperfection shape and magnitude.
- The stochastic imperfection model is able to accommodate the combined influence of imperfection shape and magnitdue. In addition to a mean estimation, the variance of ultiamte strength due to initial geometric imperfection could be evaluated.
- Based on the measured standard deviation of imperfection magnitude σ_f, the variance of the ultimate compressive strength is relatively small, with a standard deviation of 0.0086. This should be converging estimate, as shown in Figure 10.
- In three deterministic imperfection models, the CM mode is the most sensitive to the change of maximum magnitude, while the ARE mode is the least sensitive one.
- The collapse mode of the stiffened panel is independent on the initial imperfection, with a widespread elastoplastic buckling across the whole panel (Figure 11). However, the distortion nucleation in the post-collapse range is affected by the imperfection. When the determinitic imperfection is assumed, the nucleation always occurs at the central bay of the panel (Figure 12), whereas the nucleation could occur at any bay within the stiffened panel when the stochastic imperfection model is adopted.

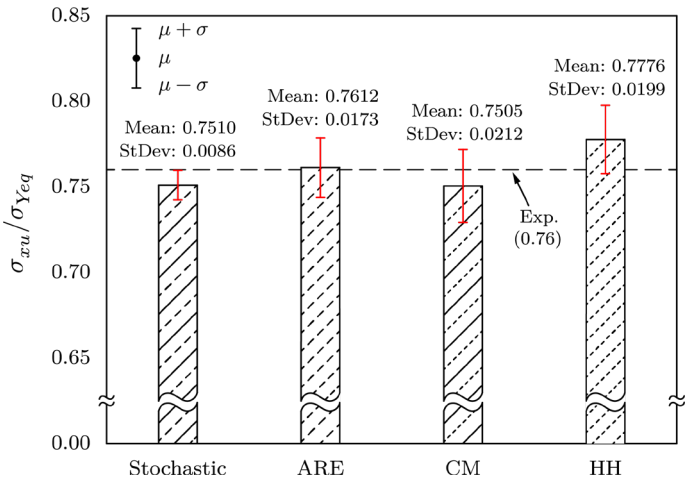

Figure 7. Comparison of the ultimate compressive strength based on different imperfection models

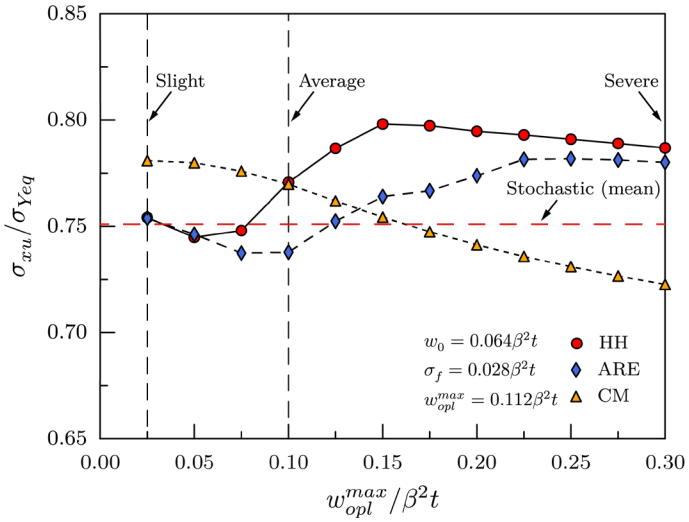

Figure 8. Relationship between the maximum distortion magnitude and the ultimate compressive strength

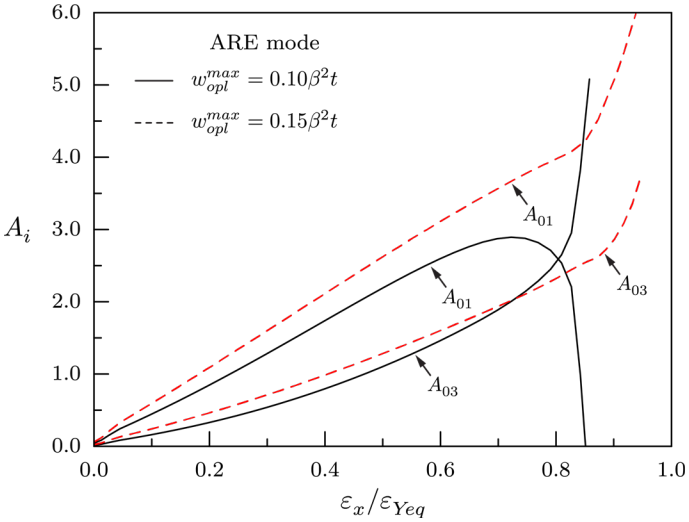

Figure 9. Decomposition of the deflection field during progressive collapse

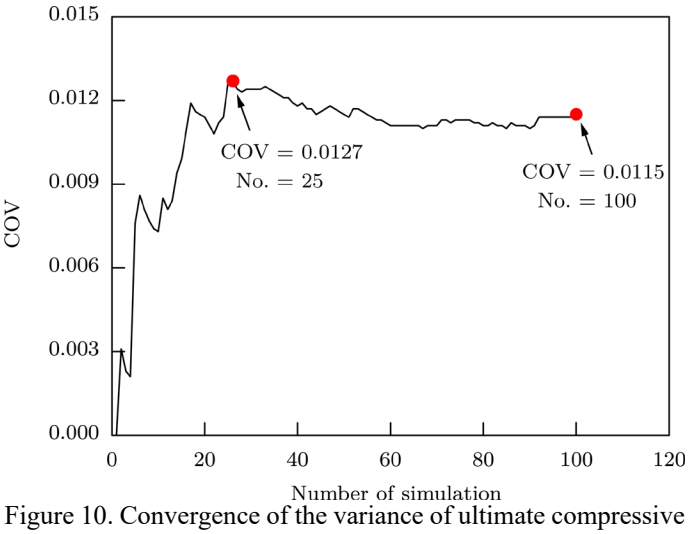

Figure 10. Convergence of the variance of ultimate compressive strength based on stochastic imperfection model

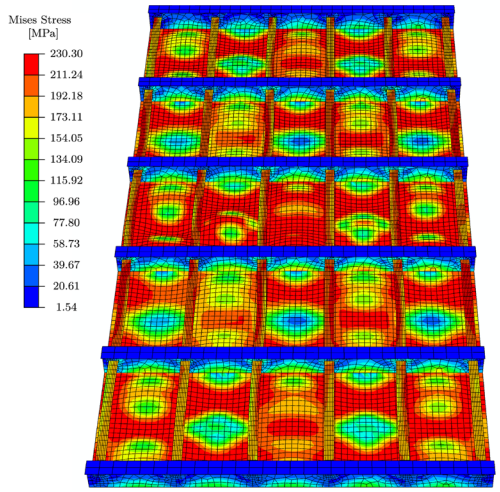

Figure 11. Collapse mode of the case study stiffened panel at ultimate limit state

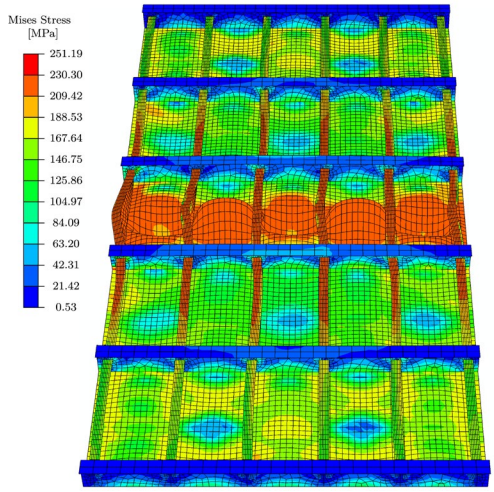

Figure 12. Collapse mode of the case study stiffened panel at post-collapse regime

5 CONCLUSIONS

This study presents a probabilistic study on the ultimate strength of stiffened panel under compression. Stochastic geometric imperfection is applied to the case study model and is compared with several well-established deterministic imperfection models. The key findings of this study are summarized as follows:

- The stochastic geometric imperfection model, utilizing the mean distortion magnitude and its variance, is a capable alternative to the deterministic imperfection model based on maximum distortion magnitude and presumed distortion shape for predicting the ultimate strength of stiffened panel.
- The stochastic imperfection model is able to account for the combined effect between distortion shape and magnitude. This is an important issue because a larger distortion magnitude may not lead to a reduction of the ultimate strength of stiffened panel. The deterministic models without this consideration may therefore give mis-leading prediction.

The present work may have implications in improving the probabilistically-based ship structure safety design. Future studies should be completed to apply the stochastic imperfection model to stiffened panels with different failure modes and to investigate the effect of standard deviation of distortion magnitude and correlation length. In addition, the effect of relative distortion between the adjacent panel should be further analyzed.

REFERENCE

Antoniou, A.C., 1980. On the maximum deflection of plating in newly built ships. Journal of ship research, 24, 31-39.

Benson, S., 2011. Progressive collapse assessment of lightweight ship structures. PhD Thesis, Newcastle University.

Benson S, Downes J, Dow RS. 2012. An automated finite element methodology for hull girder progressive collapse analysis. In Proceeding: 13th International Marine Design Conference, Glasgow, Scotland.

Benson S, Downes J, Dow RS. 2015. Overall buckling of lightweight stiffened panels using an adapted orthotropic plate method. Engineering Structures, 85, 107–117

Carlsen, C.A., Czujko, J., 1978. The specification of post-welding distortion tolerances for stiffened plates in compression. The Structural Engineer, 54A, 133-141.

Dowling, P.J., Chatterjee, S., Frieze, P.A., 1973. Experimental and predicted collapse behaviour of rectangular steel box girders. In: International Conference on Steel Box Girder Bridges, London.

Dow, R.S., Smith, C.S., 1984. Effects of localized imperfections on compressive strength of long rectangular plates. Journal of Construal Steel Research, 4, 51–76.

Georgiadis, D.G., Samuelides, M.S., 2021. Stochastic geometric imperfections of plate elements and their impact on the probabilistic ultimate strength assessment of plates and hull-girders. Marine Structures, 76, 102920.

Gordo, J.M., 2015. Effect of initial imperfections on the strength of restrained plates. Journal of Offshore Mechanics and Arctic Engineering, 137(5), 051401.

ISSC. 2012. Ultimate Strength Report. Rostock, Germany.

Kim, D.K., Kim, H.B., Park, D.H., Mohd, M.H., Paik, J.K., 2020. A practical diagram to determine the residual longitudinal strength of grounded ship in Northern Sea Routh. Ships and Offshore Structures, 15(7), 683-700.

Kim, D.K., Yu, S.Y., Lim, H.L., Cho, N.K., 2020. Ultimate Compressive Strength of Stiffened Panel: An Empirical Formulation for Flat-Bar Type. Journal of Marine Science and Engineering, 8, 605.

Kim, D.K., Pederson, P.T., Paik, J.K., Kim, H.B., Zhang, X.M., Kim, M.S., 2013. Safety guidelines of ultimate hull girder strength for grounded container ships. Safety Science, 59, 46-54.

Kim, D.K., Lim, H.L., Kim, M.S., Hwang, O.J., Park, K.S., 2017. An empirical formulation for predicting the ultimate strength of stiffened panels subjected to longitudinal compression. Ocean Engineering, 140, 270–280.

Kim, D.K., Lim, H.L., Yu, S.Y., 2019. Ultimate strength prediction of T-bar stiffened panel under longitudinal compression by data processing: A refined empirical formulation. Ocean Engineering, 192, 106522.

Kmiecik, M., 1981. Factors affecting the load-carrying capacity of plates. Technical University of Szczecin, Ship Research Institution, Report No. 115.

Li, S., Benson, S. 2019. A re-evaluation of the hull girder shakedown limit states. Ships and Offshore Structures, 14(sup1), 239-250.

Li, S, Hu, Z.Q., Benson, S., 2019. An analytical method to predict the buckling and collapse behaviour of plates and stiffened panels under cyclic loading. Engineering Structures, 199, 109627.
Li, S., Hu, Z.Q., Benson, S., 2020. Progressive collapse analysis of ship hull girders subjected to extreme cyclic bending. Marine Structures, 73, 102803.
Li, S., Kim, D.K., Benson, S., 2021. The influence of residual stress on the ultimate strength of longitudinally compressed stiffened panels. Ocean Engineering, 108839.
Merrison Committee, 1973. Inquiry into the basis of the design and method of erection of steel box bridges. HMSO, London.
Paik, J.K., 2020. Advanced structural safety studies: With Extreme Conditions and Accidents. Springer.
Paik, J.K., 2019. Ultimate limit state analysis and design of plated structures. John Wiley and Sons Ltd.
Paik, J.K., Lee, D.H., Kim, S.J., Thomas, G., Ma, M., 2019. A new method for determining the design values of wave-induced hull girder loads acting on ships. Ships and Offshore Structures, 14(sup1), 63-90.
Paik, J.K., Kim, D.K., Park, D.H., Kim, H.B., Kim, M.S., 2012. A new method for assessing the safety of ships damaged by grounding. International Journal of Maritime Engineering, 154 (A1), 1-20.
Paik, J.K., Thayamballi, A.K., Lee, J.M., 2004. Effect of initial deflection shape on the ultimate strength behaviour of welded steel plates under biaxial compressive loads. Journal of Ship Research, 48(1), 45-60.
Smith, C.S., 1981. Imperfection effects and design tolerances in ships and offshore structures. Transaction of the Institution of Engineers and Shipbuilders in Scotland, 124, 37-46.
Smith, C.S., Davidson, P.C., Chapman, J.C., Dowling, P.J., 1987. Strength and stiffness of ship's plating under in-plane compression and tension. Trans. RINA, 130, 277-294.
Smith, C.S., Anderson, N., Chapman, J.C., Davidson, P.C., Dowling, P.J., 1991. Strength of stiffened plating under combined compression and lateral pressure. Trans RINA, 134, 131-147.
Stefanou, G., 2009. The stochastic finite element method: past, present and future. Computer Methods in Applied Mechanics and Engineering, 198(9-12):1031-1051.
Shinozuka, M., Deodatis, G., 1991. Simulation of stochastic processes by spectral representation. Applied Mechanics Review. 44(4):191-204.
Tanaka, S., Yanagihara, D., Yasuoka, A., Harada, M., Okazawa, S., Fujikubo, M., Yao, T., 2014. Evaluation of ultimate strength of stiffened panels under longitudinal thrust. Marine Structures, 36, 21-50.
Ueda, Y., Yao, T., 1985. The influence of complex initial deflection modes on the behaviour and ultimate strength of rectangular plates in compression. Journal of Constructional Steel Research, 5, 265-302.
Woloszyk, K., Bielski, P.M., Garbatov, Y., Mikulski, T., 2021. Photogrammetry image-based approach for imperfect structure modelling and FE analysis. Ocean Engineering, 223, 108665.
Wong, E.W.C., Kim, D.K., 2018. A simplified method to predict fatigue damage of TTR subjected to short-term VIV using artificial neural network. Advances in Engineering Software, 126, 100-109.
Yao, T., Fujikubo, M., 2016. Buckling and ultimate strength of ship and ship-like floating structures, Elsevier.
Yi, M.S., Lee, D.H., Lee, H.H., Paik, J.K., 2020. Direct measurements and numerical predictions of welding-induced initial deformations in a full-scale steel stiffened plate structure. Thin-Walled Structures, 153, 106786.
Youssef, S.A.M., Faisal, M., Seo, J.K., Kim, B.J., Ha, Y.C., Kim, D.K., Paik, J.K., Cheng, F., Kim, M.S., 2016. Assessing the risk of ship hull collapse due to collision. Ships and Offshore Structures, 11(4), 335-350.

APPENDIX

Table A1. Coefficients of HH mode (Yao and Fujikubo, 2016)

	A_{01}	A_{02}	A_{03}	A_{04}	A_{05}	A_{06}
$1 < a/b < \sqrt{2}$	1.1158	-0.0276	0.1377	0.0025	-0.0123	-0.0009
$\sqrt{2} < a/b < \sqrt{6}$	1.1421	-0.0457	0.2284	0.0065	0.0326	-0.0022
$\sqrt{6} < a/b < \sqrt{12}$	1.1458	-0.0616	0.3079	0.0229	0.1146	-0.0065
$\sqrt{12} < a/b < \sqrt{20}$	1.1439	-0.0677	0.3385	0.0316	0.1579	-0.0149
$\sqrt{20} < a/b < \sqrt{30}$	1.1271	-0.0697	0.3483	0.0375	0.1787	-0.0199
	A_{07}	A_{08}	A_{09}	A_{10}	A_{11}	
$1 < a/b < \sqrt{2}$	-0.0043	0.0008	0.0039	-0.0002	-0.0011	
$\sqrt{2} < a/b < \sqrt{6}$	-0.0109	0.0010	-0.0049	-0.0005	0.0027	
$\sqrt{6} < a/b < \sqrt{12}$	0.0327	0.0000	0.0000	-0.0015	-0.0074	
$\sqrt{12} < a/b < \sqrt{20}$	0.0743	0.0059	0.0293	-0.0012	0.0062	
$\sqrt{20} < a/b < \sqrt{30}$	0.0995	0.0107	0.0537	-0.0051	0.0256	

Table A2. Coefficients of ARE mode

	$j = 3$	$j = 4$	$j = 5$	$j = 6$	$j = 7$	$j = 8$
A_1	1.1177	0.8410	0.7998	0.8195	0.8619	0.8122
A_j	0.2794	0.2102	0.2000	0.2049	0.2155	0.2031
A_{j+1}	0.0100	0.0100	0.0100	0.0100	0.0100	0.0100